The Effect of a Magnetic Field on a RAPET (Reaction under Autogenic Pressure at Elevated Temperature) of $MoO(OMe)_4$: Fabrication of MoO_2 Nanoparticles Coated with Carbon or Separated MoO_2 and Carbon Particles

S. V. Pol,[†] V. G. Pol,[†] V. G. Kessler,[‡] G. A. Seisenbaeva,[‡] M. Sung,[§] S. Asai,[§] and A. Gedanken*,[†]

Department of Chemistry, Bar-Ilan University, Ramat-Gan, 52900 Israel, Department of Chemistry, SLU, Box 7015, 75007 Uppsala, Sweden, and Department of Materials Processing Engineering, Graduate School of Engineering, Nagoya University, Furo-cho, Chikusa-ku, Nagoya 464-8603, Japan

Received: February 26, 2004; In Final Form: March 14, 2004

In this article, we present results of the RAPET dissociation of $MoO(OMe)_4$ at 700 °C in a closed Swagelok cell. The reaction produces molybdenum dioxide nanoparticles (20 nm) coated with carbon (20 nm). We have also carried out the same reaction under an applied magnetic field of 10 T. This reaction yielded different products. It produces a mixture of comparatively larger (50 nm) molybdenum dioxide nanoparticles and separated uncoated carbon particles (20−30 nm).

Introduction

The main product of the decomposition of $MoO(OMe)_4$ is MoO_2. Molybdenum dioxide possesses a high melting point, high electrical conductivity and is expected to have potential applications[1,2] as a catalyst, a sensor, and recording material, etc. Molybdenum oxide/carbon composite electrodes are used as electrochemical supercapacitors, and the supercapacitive behavior of the composite material was characterized by cyclic voltammetry.[3] Molybdenum oxide can exhibit pronounced photochromism and, thus, might act as an excellent photonic material for a number of technical applications.[4]

Recently Zhou et al. prepared[5] large-scale MoO_2 nanowire arrays on silicon substrates by thermal evaporation of Mo under a flow of argon gas without using any catalyst, and they also studied its field emission[6] properties. The enhanced CO tolerance of carbon-supported platinum and a molybdenum oxide anode catalyst were studied by Ioroi.[7] The influence of the active phase of molybdenum−cobalt loaded onto carbon[8] serving as a catalyst for hydrodeoxygenation reactions was studied by Ferrari. Nanocrystalline TiO_2-(MoO_3) core−shell[9] material was also investigated and reported. Recent decomposition studies of molybdenum and rhenium methoxides in a gas flow revealed the easy formation of fine powders of crystalline metal dioxides on slow heating in an inert atmosphere (nitrogen or argon).[10]

The current investigation is centered on the decomposition of a metallic oxyalkoxide in a closed cell at high temperatures. We named these reactions RAPET. The decomposition of $MoO(OMe)_4$, the precursor in the current study, was conducted both with and without a high magnetic field. To the best of our knowledge, there are no previous reports on the effect of applying a magnetic field on the synthesis of MoO_2 nanoparticles. These reactions with and without a magnetic field were carried out at 700 °C. This article shows how the magnetic field affects the products of this reaction, which in the absence of a magnetic field lead to the formation of carbon-coated MoO_2 nanoparticles. When the same reaction is conducted under an applied magnetic field of 10 T, it leads to the formation of molybdenum dioxide nanoparticles and uncoated carbon. It is interesting to understand the reason for the removal of the surface carbon shell from the MoO_2 nanoparticles. The products of the reactions with and without a magnetic field were characterized by Powder XRD, C, H, N, S analysis, EDS, TEM, HR-TEM, ESR, and BET surface area measurements.

Fabrication of Molybdenum Oxide Nanoparticles Coated with Carbon via RAPET Reactions

The fabrication of the MoO_2/C nanoparticles was carried out by introducing the $MoO(OMe)_4$ precursor (the synthesis of $MoO(OMe)_4$ has been described elsewhere[11,12]) in a 5 mL closed vessel cell. The cell was assembled from stainless steel Swagelok parts. A $^1/_2$" union part is capped on both sides by standard plugs. For these syntheses, 2 g of above precursors was introduced into the cell at room temperature under nitrogen (nitrogen filled glovebox). The filled cell was closed tightly by the other cap and then placed inside an iron pipe in the middle of the furnace. The temperature was raised at a rate of 10 °C per min. The closed cell was heated at 700 °C for 3 h. The reaction took place under the autogenic pressure of the precursor. The Swagelok was gradually cooled (∼5 h) to room temperature and opened, and a dark black powder was obtained. The total yield of product/ carbonaceous materials was about 61% for the $MoO(OMe)_4$. The material obtained is termed as "carbon coated molybdenum oxide (CCMO) nanoparticle sample". (The yield is the final weight of the product relative to the weight of the starting material.) We called this new synthesis process "reaction under autogenic pressure at elevated temperatures" (RAPET). When using this method, we have prepared monodispersed, 2.5 ± 0.05 μm size carbon spherules,[13] long carbon sausages under a magnetic field,[14] and Si-coated carbon spheres.[15]

The same procedure was carried out under a static magnetic field of 10 T, which was generated using a helium-free

* Corresponding author.
[†] Bar-Ilan University.
[‡] SLU.
[§] Nagoya University.

10.1021/jp0491360 CCC: $27.50
Published on Web 04/24/2004

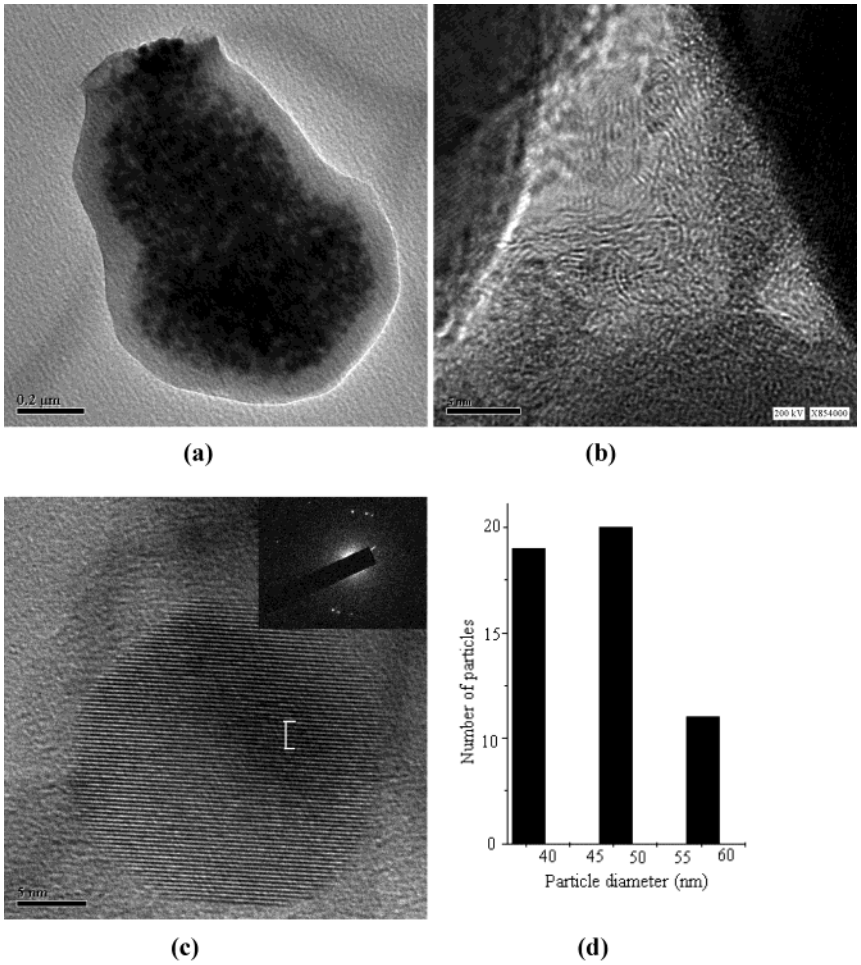

Figure 1. Transmission electron micrographs of (a) a CCMO sample, (b) carbon layers between two MoO_2 particles, (c) single particle of CCMO shown at high resolution; the insert presents its electron diffraction pattern, and (d) particle-size histogram obtained from the TEM picture a, using a Scion image software program.

superconducting magnet. The Swagelok was set in the maximum magnetic point in the bore of the magnet, where the gradient of the magnetic field was the smallest. A ceramic oven containing the Swagelok filled with 2 g of $MoO(OMe)_4$ was placed between the magnetic fields. The oven was heated and cooled, as with the reaction without a magnetic field. The yield of the product was around 60%. This sample is termed "molybdenum oxide prepared under magnetic field (MOPMF) nanoparticle sample". The yields obtained in the reaction carried out with and without the magnetic field are approximately the same.

Instrumental

XRD patterns were collected by using a Bruker AXS D* Advance Powder X-ray Diffractometer (Cu−Kα radiation, wavelength 1.5406 Å). The morphologies and nanostructure of the as-synthesized products were further characterized with a JEM-1200EX TEM and a JEOL-2010 HRTEM using an accelerating voltage of 80 and 200 kV, respectively. SAEDS (selected-area energy-dispersive X-ray analysis) of one individual particle was conducted using a JEOL-2010 HRTEM model. Samples for TEM and HRTEM were prepared by ultrasonically dispersing the products into absolute ethanol, placing a drop of this suspension onto a copper grid coated with an amorphous carbon film and then drying in air. A Scion image software program was used to measure the mean particle size of the CCMO nanoparticles. Specific surface areas were measured by the Brunauer−Emmett−Teller (BET) method at 77 K using N_2 gas as an absorbent after heating the sample at 100 °C for 1 h. The elemental analysis of the samples was carried out by an Eager 200 C, H, N, S analyzer. The Olympus BX41 (Jobin Yvon Horiba) Raman spectrometer was employed, using the 514.5 nm line of an Ar laser as the excitation source to analyze the nature of the carbon present in CCMO and MOPMF products.

Results and Discussion

We could determine the carbon and hydrogen content in the product/carbonaceous materials by an elemental analysis measurement. To study the element percent for carbon and hydrogen in the reactant and product, we calculated the element (wt.) percent in the reactants and matched this with the obtained elemental analysis data. The calculated element percent for carbon in $MoO(OMe)_4$ was 20.3% (in 2 g of precursor), while the percentage of hydrogen was 5%. The measured element percentage of carbon in the CCMO product was 6.2% (in 1.2 g of product), while the percentage of hydrogen was 0.6%. It is seen that the products show a drastic loss of carbon and hydrogen. The sample prepared in a magnetic field (MOPMF) shows only 3.5% of carbon and 0.2% of hydrogen. This means that under the magnetic field the losses of carbon and hydrogen are larger. It is suggested that the weight loss of carbon and hydrogen is due to the formation of hydrocarbons that exit in the cell as a result of the high pressure.

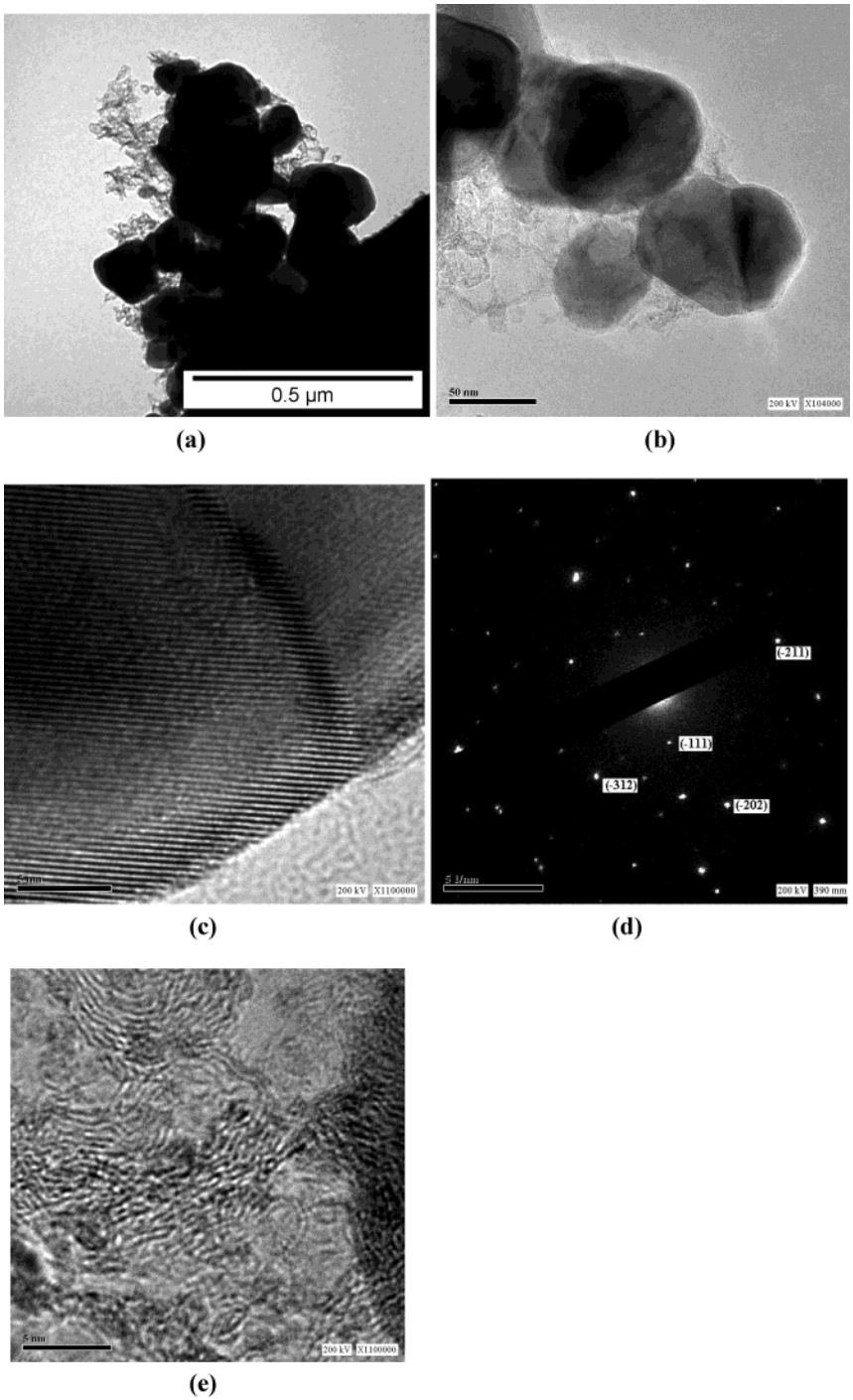

Figure 2. Transmission electron micrographs of (a) a MOPMF sample, (b) MoO_2 particles without carbon on the surface, (c) HR-TEM of a MoO_2 particle, (d) electron diffraction of same MoO_2 particle, and (e) carbon layers in a MOPMF sample.

The morphology and structure of CCMO and MOPMF samples were studied by TEM and HR-TEM measurements. Figure 1 depicts that nanoparticles having a core−shell structure are formed in the absence of a magnetic field. These nanoparticles are composed of a MoO_2 core homogeneously embedded in a carbon shell. The assignment of core to MoO_2 and the shell as carbon is based on SAEDS presented below. Due to the carbon shell surrounding the MoO_2 core, they are not agglomerated. The diameter of these MoO_2 nanoparticles is ∼20 nm, and that of the outer carbon shell is ∼20 nm. The MoO_2 core consists of hundreds of these nanoparticles (Figure 1a). This uniform 20 nm shell helps to stabilize the core and does not allow a change in its oxidation state when exposed to ambient air conditions. We assume that the dissociation of $MoO(OMe)_4$ at 700 °C leads to an atomization of the precursor into carbon, hydrogen, oxygen, and molybdenum atoms, or to the immediate formation of MoO_2 or MoO_3. If the former possibility prevails, then the molybdenum and oxygen atoms react, forming, upon cooling, a spherical MoO_2 or MoO_3 core and a shell of carbon. In the latter case, the formed MoO_2 or MoO_3 solidifies first and the solidification of the carbon follows. If the second option is correct, the RAPET reaction of $MoO(OMe)_4$ does not involve the rupture of the Mo−O bond. If MoO_3 is produced first (in either of the two options), then the carbon is responsible for its reduction. According to our interpretation, all the products of the dissociation reaction float in the gas phase and solidify right after their formation. The question is what solidifies first and what determines the order of the solidification. In the case of

the RAPET reaction of the Tetraethyl orthosilicate (TEOS), we could account for the solidification of the carbon[15] as the spherical core, both thermodynamically and kinetically. The present reaction can be explained only on a kinetic basis. Since the boiling and melting points of carbon are much higher than those of the transition metal oxides, thermodynamic carbon would, therefore, tend more easily to become a solid at 700 °C. In other words, from the thermodynamic point of view carbon would be the first to solidify and form the core, and the MoO_2 would create the shell. However, since the process is kinetically controlled, the opposite occurs. Namely, MoO_2 has a much higher solidification rate than carbon for forming the core of the composite. Carbon, having a slower solidification rate, forms the shell layer.

The disordered and ordered carbon layers (Figure 1b) were detected in an HR-TEM image. More than 50% of graphitic carbon layers (~3.5 Å) coat the surface of the MoO_2 nanoparticles. This is also proven by Raman measurements. The HR-TEM depicted in Figure 1c provides further evidence for the identification of the product as MoO_2. It illustrates the perfect arrangement of the atomic layers and the lack of defects. The measured distance between these (−111) lattice planes are 0.341 nm, which is very close to the distance between the planes reported in the literature (0.342 nm) for the monoclinic lattice of the MoO_2 (PDF: 32−671). A statistical analysis of the histogram shows that the mean size of the CCMO nanoparticles is 47.3 ± 0.1 nm. The histogram reveals (Figure 1d) a narrow size distribution of particles, which according to the TEM are monodispersed.

On the contrary, in the MOPMF product, spherical MoO_2 particles are not coated with a nanolayer of carbon (Figure 2a,b). These pictures show a mixture of two contrasting features. The dark black features are MoO_2 particles, and the pale sheets are carbon layers. The diameters of the MoO_2 particles range between 25 and 50 nm. The particles fabricated under a magnetic field are larger than those synthesized without a magnetic field. We could not find a carbon-coated MoO_2 particle on the TEM grid. The larger particles obtained under the influence of the magnetic field can be explained as being the result of the lack of carbon coating. This allows the MoO_2 particles to grow freely. The MoO_2 nanoparticles are not homogeneously coated with a carbon layer, but some contact places are observed. The HRTEM (Figure 2c) illustrates the perfect arrangement of the atomic layers and the lack of defects. The measured distance between these (−111) lattice planes are 0.346 nm, which is very close to the distance between the planes reported in the literature (0.342 nm) for the Monoclinic lattice of the MoO_2 (PDF: 32−671). However, since the distances between graphitic layers are also very similar (0.34 nm), further proof for the nature of these layers is needed. SAEDS measurements were performed.

A selected area electron diffraction (Figure 2d) was measured for the MoO_2 particle depicted in Figure 2c. The picture shows diffraction from few perpendicular planes of MoO_2 particles (related diffraction spots are given). In Figure 2e, we concentrate on the carbon sheets. The picture demonstrates that the carbon consists of mostly ordered layers. However, some disordered lattice planes of carbon are also visible. These layers are not completely graphitic but rather coal-like lattice planes, which could not be detected in XRD measurements. The interlayer spacing is ~3.53 A°, which is slightly larger than the graphitic layers. It is suggested that the existence of these layers is due to the execution of the RAPET reaction at 700 °C, which is not high enough to permit an improvement in the local order of the deposited carbon.

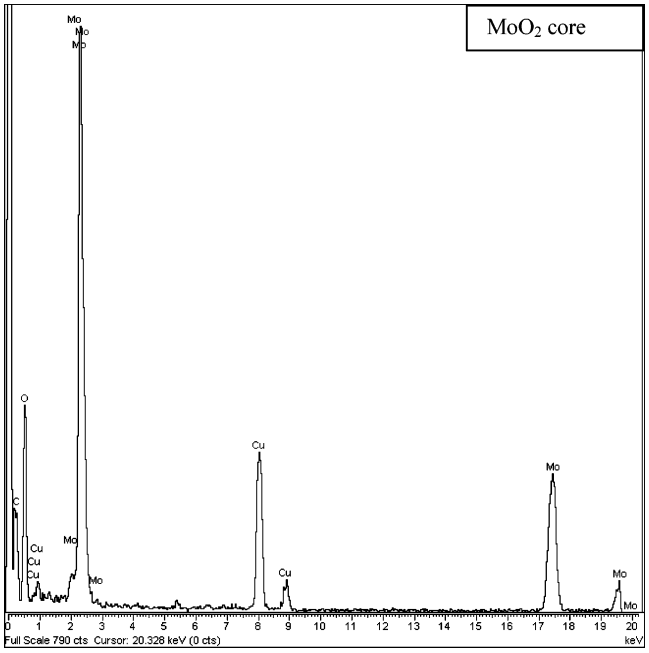

Figure 3. Selected area EDS of MoO_2 core of CCMO sample.

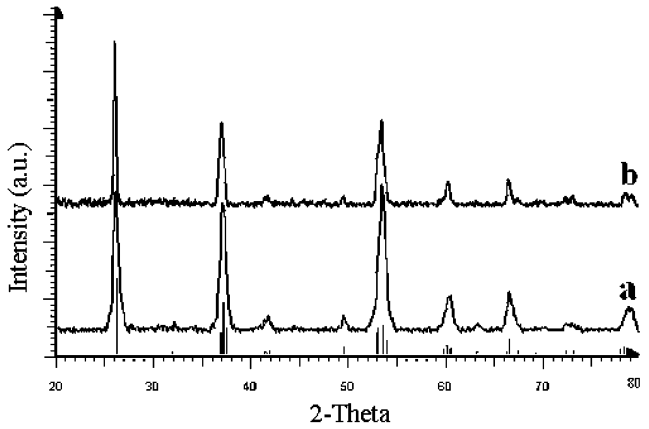

Figure 4. X-ray patterns of (a) a CCMO sample and (b) a MOPMF sample.

The SAEDS results related to the sample CCMO are presented in Figure 3. The carbon and Cu peaks originate from the TEM grid (Figure not shown). The results of a 25 nm electron beam focused on the outer surface of the MoO_2 particles show a high amount of carbon, which originated from the ~15 nm carbon shell, as well as a small amount of MoO_2 (Figure not shown). The core of the sample is MoO_2, and this is evidenced when a 25 nm electron beam is focused on the center of the CCMO particle. An intense peak assigned to MoO_2 and a weak carbon peak is detected. (Figure 3). Thus, the SAEDS results further confirm the core−shell structure of the MoO_2–C composite.

The purity, crystallinity and particle size measurements of the as-synthesized CCMO (a) and MOPMF(b) samples were examined by X-ray powder diffraction (XRD). Figure 4 shows the powder diffraction pattern collected for these products. The diffraction peaks, peak intensities, and cell parameters are in good agreement with the PDF No. 32-671 of crystalline monoclinic MoO_2. The Scherrer's equation is used to calculate the particle dimensions. The XRD peaks for the CCMO sample are broader than the MOPMF samples. The average particle size of the MoO_2 nanoparticles are ~15 nm for CCMO and 30 nm for MOPMF samples. The sample prepared without a

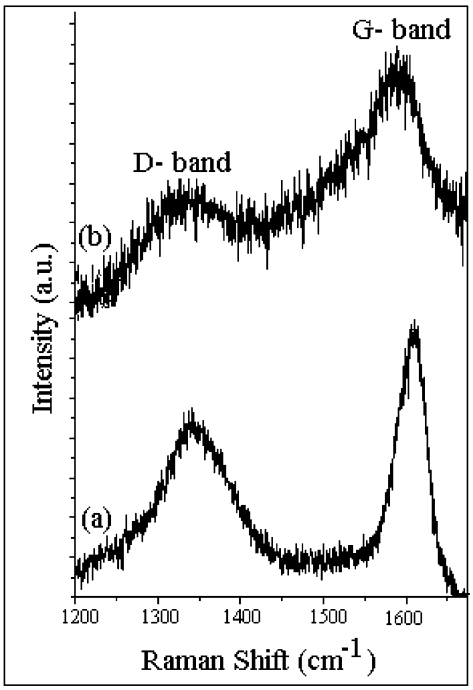

Figure 5. Raman spectra of CCMO (a) and MOPMF (b) samples.

magnetic field shows a smaller size than the sample prepared with a magnetic field. This correlates with the TEM measurements. As explained above, in the CCMO sample the coated carbon prevents the growth of MoO_2 nanoparticles.

Since the carbon is a common element found in both the CCMO and MOPMF nanoparticle samples, Raman spectroscopy measurements were performed to understand the nature of the carbon in these samples. The Micro-Raman spectra of CCMO (a) and MOPMF (b) samples are shown in Figure 5. The two characteristic bands of carbon were detected at 1341 cm^{-1} (D-band), and at 1596 cm^{-1} (G-band).[16] The intensity of the G-band, associated with graphitic carbon, is larger for both samples than the intensity of the D-band. The intensity ratios of the D- and G-bands are $I_D/I_G = 0.64$ and 0.5 for the CCMO and MOPMF samples, respectively. It is suggested that the existence of the nongraphitic layers is due to the execution of the RAPET reaction at 700 °C, which is not high enough to permit an in improvement in the local order of the deposited carbon.

The measured surface area for the CCMO and MOPMF products are 16 and 16.5 m^2/g, respectively. The particle size of the CCMO product was smaller than the MOPMF, but the surface area of both materials is same. For the MOPMF sample, the results represent a measurement of the carbon surface as well as the MoO_2 nanoparticles.

Electron paramagnetic resonance (EPR) spectra of the CCMO and MOPMF samples taken at room temperature are different. A complex spectrum depicting at least two derivative-shapes/lines is observed for CCMO (Figure 6a), while for the MOPMF a strong narrow ESR signal (Figure 6b) is detected. The *g*-factor is equal to 2.002319 for an unbound electron.The CCMO sample showed two ESR signals at *g*-values of 2.0066 and 2.0846, while the MOPMF sample shows a *g*-value of 2.0453. The origin of the EPR signal is the carbon, for which abundant literature[17−19] is available associating the signal with free radicals on the surface of carbon. We attribute the rich spectrum obtained for CCMO to the interaction of the MoO_2 with the carbon-free radicals. This leads to the splitting of the carbon signal. On the other hand, for the MOPMF sample this interaction is nonexistent due to the lack of contact between the carbon and the MoO_2.

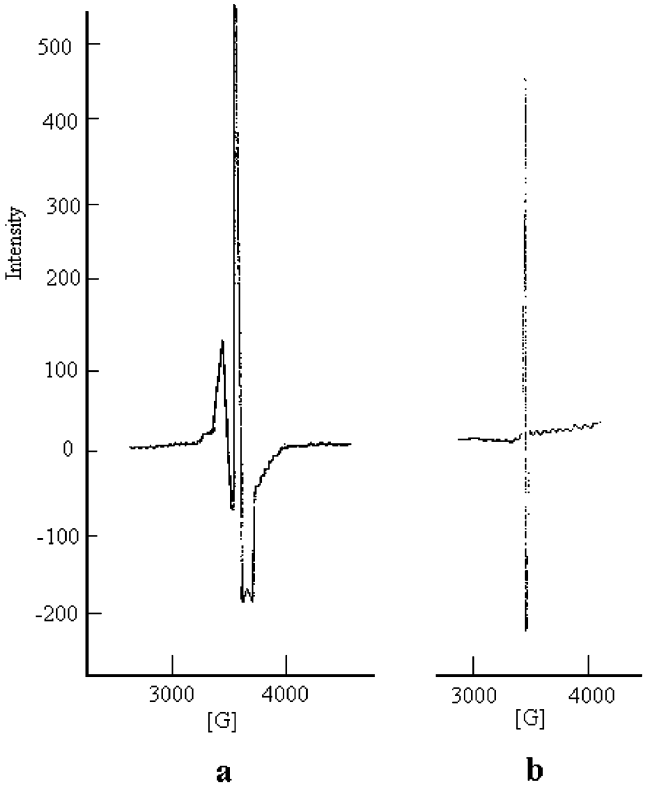

Figure 6. Electron paramagnetic resonance spectra of the CCMO (a) and MOPMF (b) samples taken at room temperature.

Proposed Mechanism

A similar RAPET reaction, under the same conditions, is conducted for Vanadium (V) oxytriethoxide [$VO(OC_2H_5)_3$] in a Swagelok at 700 °C, for 3 h, with and without a magnetic field. In both reactions, the thermal decomposition produces a core−shell nanostructure, namely, carbon coated on vanadium oxide, where the obtained nanosized V_2O_3 is the core and the carbon is produced as a uniform shell of ∼15 nm. Unlike $MoO(OMe)_4$, we could not observe any morphological change on the application of the magnetic field for $VO(OC_2H_5)_3$. Our interpretation focuses on the application of a magnetic field, since only then do differences between V and Mo alkoxides exist. Without a magnetic field the products are similar for both transition metals. The reason separate particles of carbon and MoO_2 are observed upon the application of magnetic field is due to a magnetic rejection between the MoO_2 and the carbon in the transition state. Pure monoclinic MoO_2 crystals are weakly paramagnetic.[20] The carbon surface is also known to be paramagnetic,[17−19] as demonstrated by ESR measurements. Upon cooling, the MOPMF product fabricated in a magnetic field at 700 °C/3 h, causes the MoO_2, which solidifies first, to reject any approaching carbon moiety. This results in the separation of carbon and the MoO_2 particles.

References and Notes

(1) Yao, J. N.; Hashimoto, K. H.; Fujistima, A. *Nature* **1992**, *355*, 624.

(2) Gulino, A.; Parker, S.; Jones, F. H.; Egdell, R. G. *Chem. Soc. Faraday Trans.* **1996**, *12*, 2137.

(3) Sugimoto, W.; Ohnuma, T.; Murakami, Y.; Takasu, Y. *Electrochem. Solid State Lett.* **2001**, *4* (9), A145.

(4) He, T.; Yao, J. N. *J Photochem. Photobiol. C−Photochem. Rev.* **2003**, *4* (2) 125.

(5) Zhou, J.; Xu, N. S.; Deng, S. Z.; Chen, J.; She, J. C. *Chem. Phys. Lett.* **2003**, *382* (3−4), 443.

(6) Zhou, J.; Xu, N. S.; Deng, S. Z.; Chen, J.; She, J. C.; Wang, Z. L. *Adv. Mater. 15* (21), **2003**, 1835.

(7) Ioroi, T.; Yasuda, K.; Siroma, Z.; Fujiwara, N.; Miyazaki, Y. *J. Electrochem. Soc.* **2003**, *A1225*.

(8) Ferrari, M.; Delmon, B.; Grange, P. *Microporous Mesoporous Mater.* **2002**, *56* (3), 279.

(9) Elder, S. H.; Cot, F. M.; Su, Y.; Heald, S. M.; Tyryshkin, A. M.; Bowman, M. K.; Gao, Y. A.; Joly, A. G.; Balmer, M. L.; Kolwaite, A. C.; Magrini, K. A.; Blake, D. M. *J Am. Chem. Soc.* **2000**, *122* (21), 5138.

(10) Seisenbaeva, G. A.; Sundberg, M.; Nygren, M.; Dubrovinsky, L.; Kessler, V. G. *Mater. Chem. Phys.*, in press (no. MAC_kesslervg_20040108/1).

(11) Seisenbaeva, G. A.; Werndrup, P.; Kloo, L.; Kessler, V. G. *Inorg. Chem.* **2001**, *40*, 3815.

(12) Kessler, V. G.; Mironov, A. V.; Turova, N. Y.; Yanovsky, A. I.; Struchkov, Y. T. *Polyhedron* **1993**, *12*, 1573.

(13) Pol, V. G.; Motiei, M.; Gedanken, A.; Calderon-Moreno, J.; Yoshimura, M. *Carbon* **2004**, *42*, 111.

(14) Pol, V. G.; Pol, S. V.; Gedanken, A.; Sung, M.; Asai, S. *Carbon*, submitted for publication.

(15) Pol, V. G.; Pol, S. V.; Gofer, Y.; Calderon-Moreno, J.; Gedanken, A. *J. Mater Chem.* **2004**, *14*, 966.

(16) Dresselhaus, M. S.; Dresselhaus, G.; Pimenta M. A.; Eklund, P. C. In *Analytical Application of Raman Spectroscopy*; Pelletier, M. J., Ed.; Blackwell Science: Oxford, 1999; Chapter 9.

(17) Mrozowski, S. *Carbon* **1979**, *17* (3), 227.

(18) Mrozowski, S. *Carbon* **1982**, *20*, 303.

(19) Mrozowski, S. *Carbon* **1988**, *26*, 521.

(20) Ben-Dor, L.; Shimony, Y. *Mater. Res. Bull.* **1974**, *9* (6), 837.